Vol. 231: 215–228, 2002 | MARINE ECOLOGY PROGRESS SERIES
Mar Ecol Prog Ser | Published April 22

Bioaccumulation of inorganic and methylated mercury by the gills of the shore crab *Carcinus maenas*: transepithelial fluxes and histochemical localization

J. M. Laporte[1], J. P. Truchot[2,*], N. Mesmer-Dudons[1], A. Boudou[1]

[1]Laboratoire d'Ecophysiologie et d'Ecotoxicologie des Systèmes Aquatiques (LEESA), UMR CNRS 5805, Station marine, 33120 Arcachon, France

[2]UFR de Sciences Biologiques, Université Bordeaux 1, Avenue des Facultés, 33405 Talence Cedex, France

ABSTRACT: In order to better understand the role of the gills in the accumulation of contaminants, branchial uptake and bioaccumulation of inorganic ($HgCl_2$) and monomethylmercury (CH_3HgCl) were quantified in the shore crab *Carcinus maenas*, using living animals and an *in vitro* perfused gill preparation exposed to 50 µg l^{-1} of either chemical forms in the external medium. In addition, localization of accumulated mercury was studied using the histochemical autometallographic technique by both light and electron microscopy. Gill tissue strongly accumulated either inorganic or methylated mercury at similar levels *in vitro* and *in vivo*. For both chemical forms of the metal, only about 1% of the total mercury input was recovered in the effluent fluid from *in vitro* perfused gills and could thus be considered available to distribute inside the animal via the circulatory system. Inorganic Hg was histochemically found to be accumulated at 2 markedly different locations in the gills: at the cuticular surface in direct contact with the contaminated medium and at high local levels in the central vacuole of gill nephrocytes. Although also present at these 2 locations, methylmercury was distributed more diffusely and more evenly in all cells. These results suggest that the high affinity of gill tissue for both forms of mercury may confer on this organ the role of an external barrier strongly limiting the invasion of the metal toward other compartments of the body.

KEY WORDS: Mercury and methylmercury · Perfused crab gills · Transbranchial fluxes · Autometallographic localization

INTRODUCTION

Most of the studies devoted so far to mercury contamination of aquatic animals have been concerned with the levels of metal accumulation in various species under different environmental conditions. Toxic effects and the capacity of the metal for biomagnification along food chains have also been well documented (Jackson 1991, Parkman & Meili 1993, Suedel et al. 1994, Stein et al. 1996, 1998, Boudou & Ribeyre 1998, Lawson & Mason 1998, Morel et al. 1998). However, knowledge of organism/mercury interactions and especially of the mechanisms leading to bioaccumulation and toxicity remain fragmentary. Among these processes, the step of metal uptake is obviously a crucial issue in aquatic organisms. It is commonly thought that the main route of entry of trace metals from the ambient medium is the gill epithelium, and recent studies have shown that this is indeed the case for mercury in crabs (Barradas & Pequeux 1996, Pequeux et al. 1996). Furthermore, a number of other studies indicate that the gill tissue of several crustacean species is able to accumulate very high amounts of mercury following

*Corresponding author.
E-mail: truchot@ufrbiol-bx1.u-bordeaux.fr

direct contamination from the ambient water (McLusky & Bryant 1986, Canli & Furness 1995, Wright 1995, Bianchini & Gilles 1996, Laporte et al. 1996, 1997). In the shore crab *Carcinus maenas* for example, 15 d exposure to 1 µg l^{-1} of either inorganic or methylmercury resulted in gill bioconcentration factors of up to 1500–3000, corresponding to gill metal concentrations that were 10 to 50 times higher than in the carapace and internal organs. So, although the gills account for no more than 1% of the shore crab body weight, they could accommodate as much as 33% of the total body burden of inorganic mercury (Laporte et al. 1997).

The reasons for such a marked gill organotropism as well as its possible functional significance are not known. Because it is tempting to think that it could confer on the gill the role of a protective barrier limiting access of the metal to internal tissues in the case of direct contamination, it would be essential to determine which proportion of the metal taken up is retained in the gill tissue and which amount is left free to distribute inside the organism.

The initial aim of the present study performed on the shore crab *Carcinus maenas* was to assess the efficiency of the gill in retaining mercury taken up from the surrounding medium. This was done by using the isolated and perfused gill technique, which enabled us to quantify the transepithelial fluxes of Hg during a short period (2 h) while measuring the total accumulation in the organ. In a second step, we focused on the fine localization of mercury in gill tissues of *C. maenas*, a widespread species the gill structure of which has been extensively studied (Compère et al. 1989, Goodman & Cavey 1990, Taylor & Taylor 1992, Lawson et al. 1994). We applied the autometallographic histochemical technique (Danscher 1984, Soto et al. 1996) to visualize the cellular localization of Hg in the gills, using both light and transmission electron microscopy. As it is commonly assumed that inorganic Hg and methylmercury differ in bioavailability and uptake mechanism, we additionally tried to differentiate tissue Hg localization when crabs were contaminated with either inorganic and organic forms of the metal in the ambient water.

MATERIALS AND METHODS

Crabs. Adult male crabs (33 ± 4 g fresh weight) obtained from local fishermen from the Arcachon basin were laboratory-maintained for at least 3 wk in 40-l tanks (8 crabs per tank) of aerated and filtered artificial seawater (Instant Ocean) at 33‰ salinity and 15°C. Such an acclimatization period in the laboratory was deemed necessary to obtain crabs with gills as clean as possible. Indeed, freshly caught crabs can have sediment deposits at the surface of their gills. For the same reason, only crabs with a light 'green' color that had molted only a few weeks previously were used in experiments.

Contamination experiments. In an initial step designed to study the bioaccumulation capacity of the gills, a batch of 18 crabs was used. They were placed individually in glass aquaria containing 3 l of aerated artificial seawater at 15°C and kept there for 1 d to attain a settled condition and avoid unwanted stress reactions such as hyperactivity and increased gill ventilation which could influence metal accumulation. Then, 2 groups of 6 crabs were treated with Hg(II) ($HgCl_2$, Merck) or MeHg(II) (CH_3HgCl, Merck) added as concentrated solutions to reach a metal concentration of 50 µg l^{-1} in the medium. Exposure duration was either 0.5 or 2 h for each subgroup of 3 contaminated crabs, the 2 remaining uncontaminated subgroups of 3 crabs serving as controls. Then, the crabs were killed and posterior gill pairs (number 7 and 8) were removed, weighed and stored at –20°C before being digested with concentrated HNO_3 and analyzed for Hg content using cold vapor atomic fluorescence spectroscopy (SFA-Merlin-Plus, Seven Oaks, UK) (Jones et al. 1995). Metal concentrations measured in gills from contaminated crabs were corrected by subtracting the values obtained in controls (mean value = 22 ng g^{-1} fresh weight). This slight correction represents only 0.59 ± 0.35% of the total mercury accumulated in the gills at the end of the experiment.

Gill perfusion method. Posterior gills (number 7 and 8) were quickly and carefully removed from cold-anesthetized crabs by cutting the gill shaft at its base. Exposure of the organ to air was avoided as much as possible, and all the phases of preparation were performed in a clean artificial medium (see composition below) with adequate osmotic properties. The basis of the method consisted in the replacement of hemolymph, the natural convection medium in the live crab, by an artificial system allowing precise control of the external and internal media (Pierrot et al. 1995). PTFE catheters were introduced in both afferent and efferent channels of the gill and sealed in place with a small amount of cyanoacrylate glue. A peristaltic pump provided a steady flow (15 ml h^{-1}) of the artificial perfusion medium (ionic composition: 560 mM NaCl, 15 mM $CaCl_2$, 15 mM KCl, 20 mM $MgSO_4$, 10 mM KH_2PO_4, pH 7.9). The gill was placed in a jar thermostatted at 15°C and containing 100 ml of the same solution that was either left uncontaminated (control) or enriched with a metal concentration of 50 µg l^{-1} (HgII or MeHg). This external medium was air-equilibrated before metal addition and agitated with a magnetic bar throughout the experiment to simulate natural convec-

tion of the water at the gill surface. The effluent fluid from the perfused gill was collected in a storage flask during an experiment that lasted 0.5 or 2 h, a duration compatible with the survival time of such an *in vitro* perfused tissue (Pierrot et al. 1995). The reliability of the preparation was checked by comparing the observed perfusion flow to the value nominally delivered by the pump, so that any difference indicative of a leak in the system could be detected.

At the end of the experiments, the gill and the collected perfusion fluid samples were weighed, stored in Teflon vials and frozen until the analysis of their Hg content as described above. Transbranchial fluxes were calculated from the amount of mercury found in the collected fluid after 2 h perfusion. Total Hg(II) or MeHg uptake was obtained by summing these transbranchial fluxes and the amounts of mercury accumulated in gill tissue at the end of the experiment. The proportion of the metal entering the organ and effectively reaching the internal circulatory system could thus also be calculated. The accumulation of mercury in perfused gills was corrected for control values as above and statistically compared with a *t*-test to values obtained in contaminated live crabs.

Preparation of gill samples for microscopy. Histochemical localization of Hg by autometallography was performed on posterior gills (number 7 and 8) obtained from uncontaminated crabs as well as from live animals exposed to metal for 2 h at 50 µg l^{-1} (HgII or MeHg), with a protocol similar to the one described above. The total number of examined gills reached about 50 for light microscopy and 30 for electron microscopy.

Gill tissue was fixed by both immersion and perfusion for 15 min using a solution containing 5% glutaraldehyde (Grade I, Sigma), 0.1 M sodium cacodylate buffer (pH 7.9) (Sigma) and enough NaCl to get an osmolality of 1100 mOsm, as measured by vapor pressure osmometry (Wescor 5500). Before fixation, half of the samples to be examined by light microscopy had been perfused with a 0.1% sodium selenide solution (with adequate pH and osmolality) for 10 min while being immersed in the same solution. The other half was perfused with fixative solution only. Samples obtained for electron microscopy were systematically perfused with the selenium solution. After perfusion, the gills were cut into small pieces and left for 12 h in the fixative at 4°C before being rinsed in cacodylate-NaCl. Samples for light microscopy were dehydrated in toluene and embedded in paraffin. Sections cut at 10 µm were placed on glass slides and covered with a thin layer of gelatin (5%, Type A, Sigma). Pieces to be prepared for electron microscopy were first postfixed in 1% OsO_4, then dehydrated in propylene oxide and embedded in Araldite. Ultrathin sections were cut at 40 nm, collected on nickel grids and immediately gelatinized. For both light and electron microscopy, no staining other than the autometallography reaction was applied.

Autometallography. Autometallography is a very sensitive technique for detection of sulfide-bound metal groups (Danscher 1984, Danscher & Møller-Madsen 1985, Newman & Jasani 1998, Braeckman & Raes 1999). These groups act as catalysts for reduction of Ag^+ ions to Ag atoms that themselves aggregate, allowing further catalysis, amplification of the reaction and deposition of easily detectable silver grains. Due to its high affinity for selenium, mercury could be detected not only as bound to sulfide groups but also as selenide complexes, which also act as catalysts. Thus, prior treatment of the samples with selenium salts could reveal additional mercury not initially bound to thiol groups.

The routine of the method used in this work was based on that of Danscher & Møller-Madsen (1985) with further improvements (Baatrup & Doving 1990, Danscher et al. 1994, Marigomez et al. 1996, Soto et al. 1998). Sections for light or electron microscopy were incubated for exactly 1 h at a controlled temperature of 26 ± 0.2°C in complete darkness in a developer solution containing arabic gum (50%, Sigma), 0.1 M citrate buffer pH 7.9 (citric acid, Prolabo; sodium citrate, Sigma), 0.08 M hydroquinone (photographic grade, Sigma) and 3 mM silver lactate (lactic acid, silver salt, Sigma). After rinsing, the reaction was stopped by dipping in sodium thiosulfate 0.1 M (photographic grade, Sigma) for 30 s. This procedure was strictly followed for all samples in order to accurately standardize reaction times and arrive at the best comparable results. Observations were conducted either on a BX50 Olympus optical microscope or on a Hitachi H-600 transmission electron microscope.

RESULTS

Mercury accumulation and gill transbranchial fluxes

Fig. 1 summarizes the data obtained for Hg accumulation in the gills after 0.5 and 2 h exposure to a concentration in water of 50 µg l^{-1} of inorganic and organic forms of mercury, either *ex vivo* (isolated and perfused gill) or *in vivo* (live crab). In both conditions, gill metal levels were significantly higher after 2 h compared to 0.5 h. After 2 h, inorganic Hg accumulation amounted to 6324 ng Hg g^{-1} in the perfused gill and 6573 ng Hg g^{-1} in the gill contaminated *in vivo*. MeHg uptake was significantly higher at 8316 ng Hg g^{-1} for *ex vivo* and 9316 ng Hg g^{-1} for *in vivo* exposure after 2 h. Although the small number of observations (N = 3 or 4) limits the validity of statistical comparisons, no significant differ-

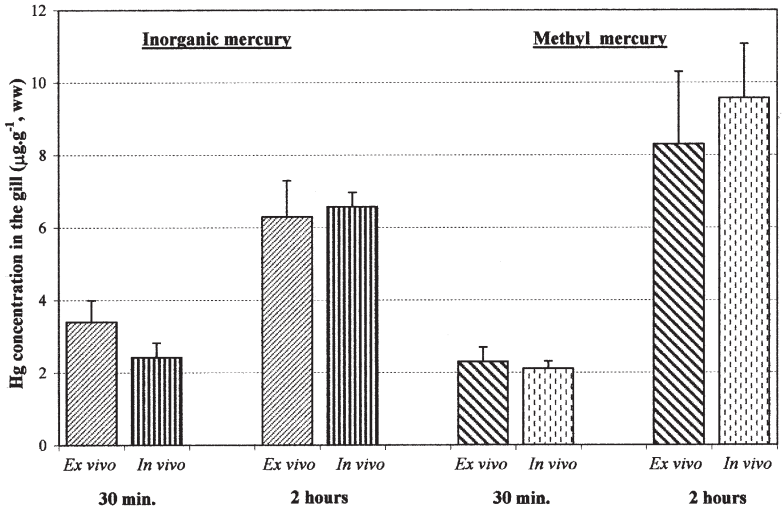

Fig. 1. *Carcinus maenas.* Hg concentrations in posterior gills (numbers 7 and 8) of crabs contaminated *ex vivo* (perfused gills) or *in vivo* (live crabs) with inorganic (HgII) and organic (monomethylated form) mercury at a concentration in water of 50 µg l^{-1} for 30 (left) and 120 (right) min. Mean ± standard deviation from 4 (*ex vivo*) or 3 (*in vivo*) experiments. Differences between *ex vivo* and *in vivo* values are not significant ($p > 0.05$). The values in control animals or perfused gills (22 ng Hg g^{-1} on average) have been subtracted from the results

ences could be found between the *ex vivo* and *in vivo* exposures for either chemical form. This result might suggest that the isolated preparation is an acceptable model for the study of acute gill contamination by mercury. In both *ex vivo* and *in vivo* experiments, accumulation seemed to begin more slowly for organic mercury, but reached higher concentrations in gill tissue than for the inorganic form after 2 h. Despite a very short exposure time, bioconcentration factors amounted to high values of 100 to 200, confirming the very high capacity of crustacean gills for mercury accumulation.

Measured transbranchial fluxes of mercury were very low. Table 1 shows that only 82 ± 26 and 60 ± 25 ng Hg g^{-1} gill fresh weight of inorganic Hg and MeHg, respectively, were collected from the efferent canal during the 2 h perfusion experiment. Amounts of methyl- and inorganic mercury crossing the gill barrier were not significantly different. Total uptake (Hg accumulated in the gill + Hg recovered in the perfusate) was slightly higher for the methylated form of the metal. Mercury recovered in the perfusate represented only 1.2 % for inorganic Hg and 0.7 % for MeHg of the total influx of Hg in the gill, the remainder (around 99 %) being trapped in the gill tissue.

Autometallographic localization of mercury in gill tissue

The gill of crabs is of the phyllobranchiate type and comprises a flattened gill shaft containing afferent and efferent channels and bearing rows of gill lamellae on each side. Lamellae are bordered by 2 sheets of cuticle and epithelium linked together by pillar cells crossing hemolymph lacunae. Pillar cells also hold up a central sheet of conjunctive tissue called the intralamellar septum. There are 5 main cell types in the gill lamellae (Goodman & Cavey 1990, Taylor & Taylor 1992): epithelial cells that are either thin (chief cells) or thick and mitochondria-rich (striated cells), pillar cells, nephrocytes and glycocytes in the lamellar septum and gill shaft.

Fig. 2 shows representative aspects of gill mercury accumulation as observed by light microscopy on sections not previously treated with selenium salts. In the absence of any histological staining, sections from control, uncontaminated gills (Fig. 2a, b) display low-contrast pictures on which the general structure of the gill lamellae and shaft remains visible. There are no obvious silver deposits on these sections, indicating that no or only very little mercury (or any other reactive metal) was present. By contrast, gills from crabs exposed to inorganic mercury (Fig. 2c,d) clearly exhibit positive reactions, but with a very heterogeneous distribution of the metal. Very dense globular deposits, either grouped or in isolation, are apparent along the intralamellar septum as well as inside the gill shaft, but they appear to remain well localized, leaving many cellular structures free of contamination. Another location for metal deposits appears at the surface of gill lamellae as a thin and irregular lining, how-

Table 1. *Carcinus maenas*. Accumulation, transepithelial fluxes, total uptake and percentage of mercury reaching the internal circulation in the perfused gills of *crabs* exposed to 50 µg l^{-1} of inorganic or methylHg in water during 2 h (N = 4; mean values ± standard deviation). Accumulation values have been slightly corrected by subtracting values measured in control animals (22 ng g^{-1})

	Inorganic Hg	MethylHg
A — Accumulation in the gill tissue (ng Hg g^{-1}, 2 h)	6324 ± 968	8316 ± 1673
B — Transepithelial flux (ng Hg g^{-1}, 2 h)	82 ± 26	60 ± 25
Total uptake (ng g^{-1}, 2 h) (A+B)	6406 ± 974	8376 ± 1602
Percentage of mercury reaching the internal circulation [B/(A+B)] (%)	1.28 ± 0.18	0.72 ± 0.13

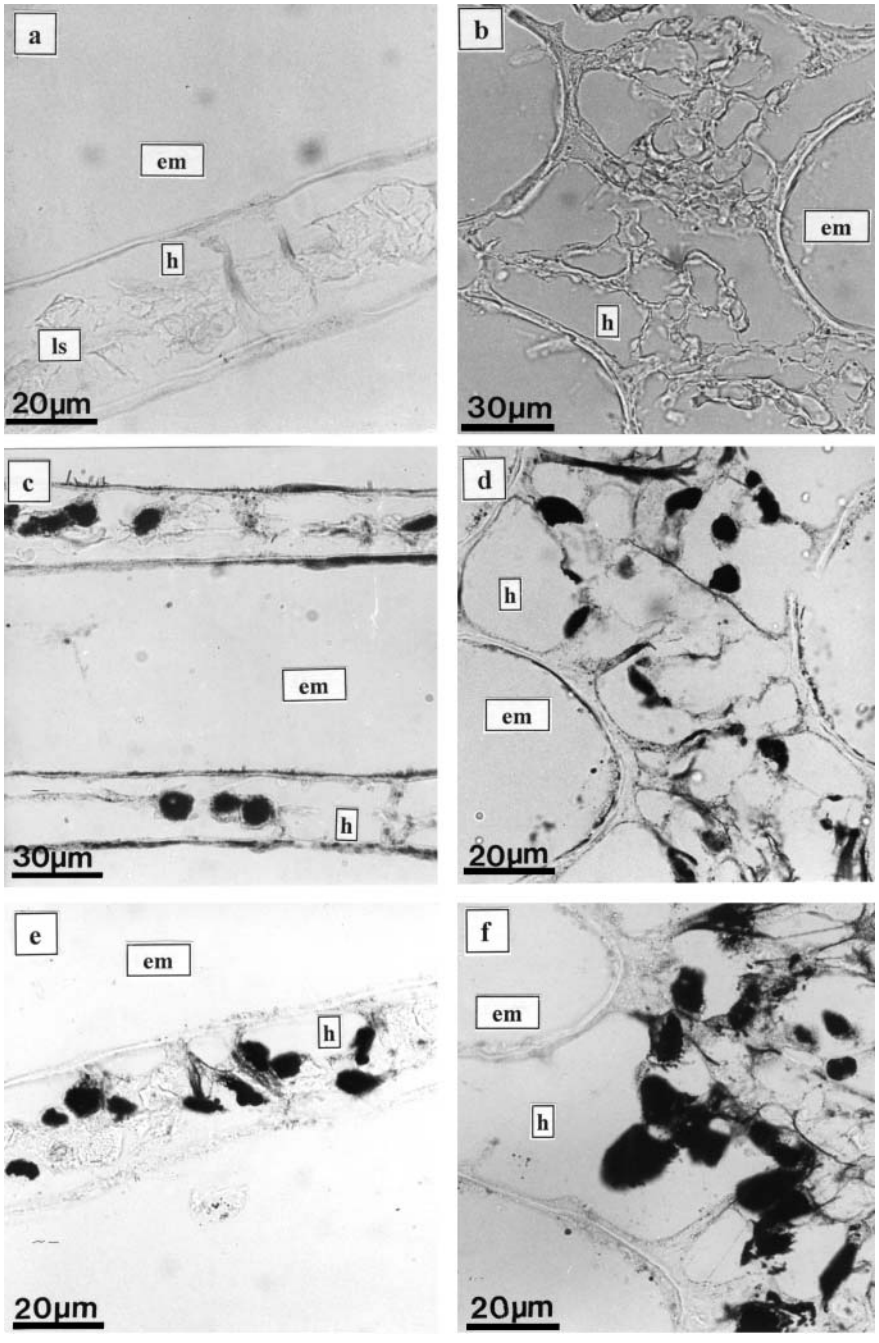

Fig. 2. *Carcinus maenas.* Light microscopic sections of gills (numbers 7 and 8) treated by autometallography. Gill lamellae are shown in left panels and gill shaft in right panels. (a,b) Uncontaminated control crabs. Despite low contrast due to the absence of staining, the cuticle and epithelial sheets, the intralamellar septum and 2 pillar cells are easily recognized on the lamellar section. No silver deposits are visible on these control sections. (c,d) Crabs contaminated by 2 h exposure to inorganic mercury (50 µg l^{-1}). Dense granules within the lamellar septum and gill shaft are labelled. Silver deposits are also visible on the cuticular surface. (e,f) Crabs contaminated by 2 h exposure to methylmercury (50 µg l^{-1}). Dense granules within the lamellar septum and gill shaft are labelled, but only few silver deposits are visible on the cuticular surface. (em, external medium; h, hemolymph space; ls, lamellar septum)

ever not reaching the underlying epithelium which remains clean. In gills of crabs contaminated with methylmercury (Fig. 2e,f), a similar distribution of dense globular silver deposits was observed along the lamellar septum and within the gill shaft, but the cuticular lining of the lamellae was practically free of metal.

Localization of mercury in sections from gills treated with sodium selenide is shown in Fig. 3. While no silver deposits could be seen in uncontaminated control crabs (Fig. 3a,b), mercury detection is clearly enhanced compared to selenide-untreated, Hg-contaminated gills. Not only dense globular deposits are present, but, especially following inorganic mercury exposure (Fig. 3c,d), all cellular structures appear diffusely marked. Silver deposits are also present on the cuticular lining after methylmercury contamination (Fig. 3e,f).

Aspects of autometallographic mercury detection using transmission electron microscopy are presented in Figs. 4, 5 & 6. Sections of gill lamellae from uncontaminated control crabs illustrate some cytological details. The cuticle and underlying chief cells are seen on Fig. 4 a,b. The cuticle clearly comprises 3 layers: a thin epicuticle, an exocuticle and a multilayered endocuticle of variable thickness according to the molt stage of the animal. It is often (but not always, Fig. 4b) coated with a biofilm containing detritus, algae and bacteria. Fig. 4c shows a pillar cell anchored to the cuticle. Nephrocytes, sometimes also called podocytes, are clearly seen on Fig. 4d. These are large, spherical cells generally found attached to the lamellar septum and within the gill shaft, with a large, dense central vacuole and a peripheral network of small, regular, finger-like processes or pedicels connected by a thin diaphragm and separated from the hemolymph space by a basement membrane. In all these control sections, silver grains are very scarce and almost homogeneously distrib-

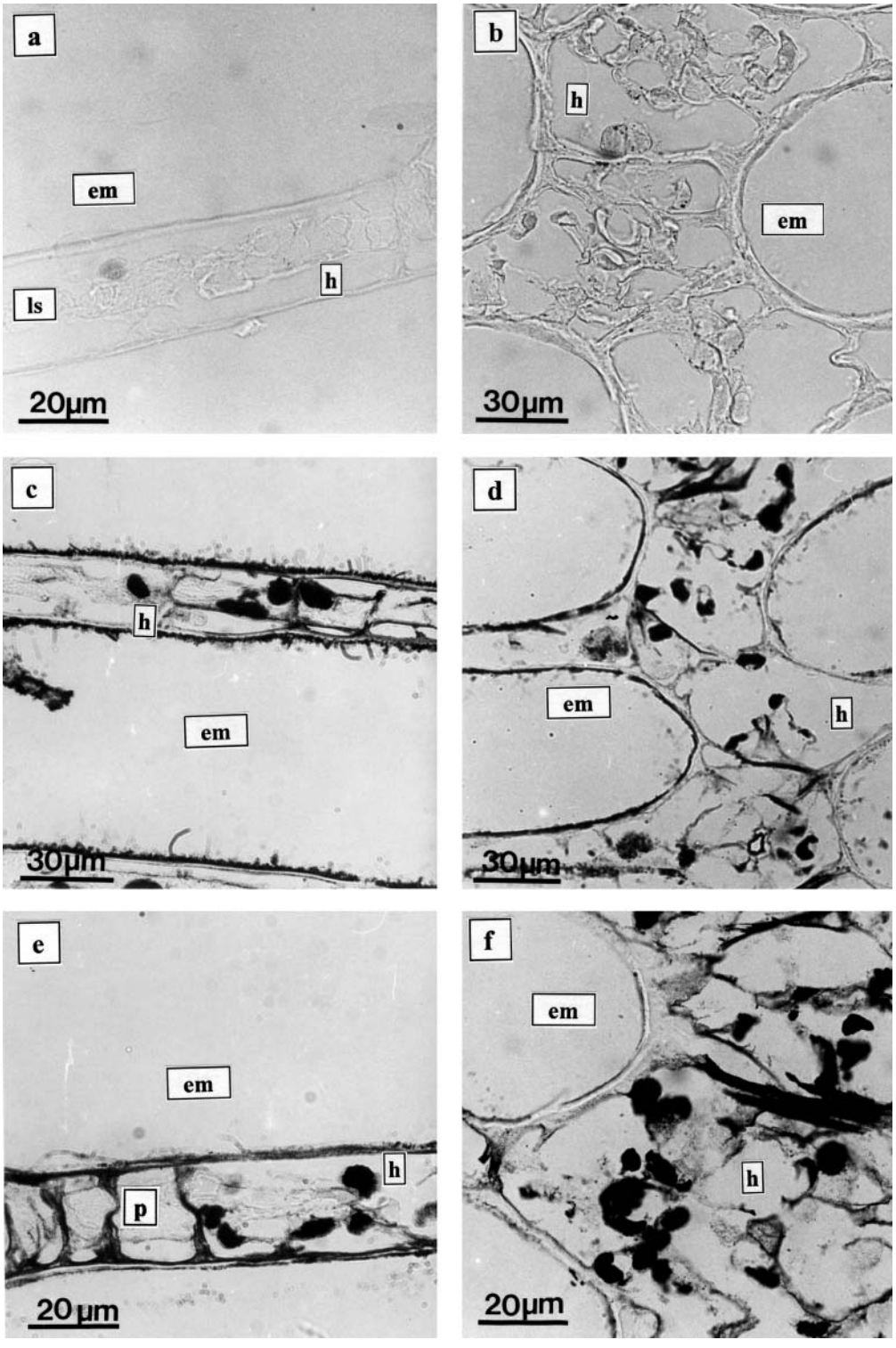

Fig. 3. *Carcinus maenas.* Light microscopic sections of gills (numbers 7 and 8) preincubated in sodium selenide and further treated by autometallography. Gill lamellae are shown in left panels and gill shaft in right panels. (a,b) Control samples with no silver deposits visible. (c,d) Crabs contaminated by 2 h exposure to inorganic mercury (50 µg l^{-1}) . Dense granules within the lamellar septum and gill shaft are labelled. Silver deposits are also visible on the cuticular surface. All other cellular structures display a lighter labelling. (e,f) Crabs contaminated by 2 h exposure to methylmercury (50 µg l^{-1}) . Dense granules within the lamellar septum and gill shaft are labelled. Fewer silver deposits are visible on the cuticular surface while all other cellular structures display a lighter labelling. (em, external medium; h, hemolymph space; ls, lamellar septum; p, pillar cells)

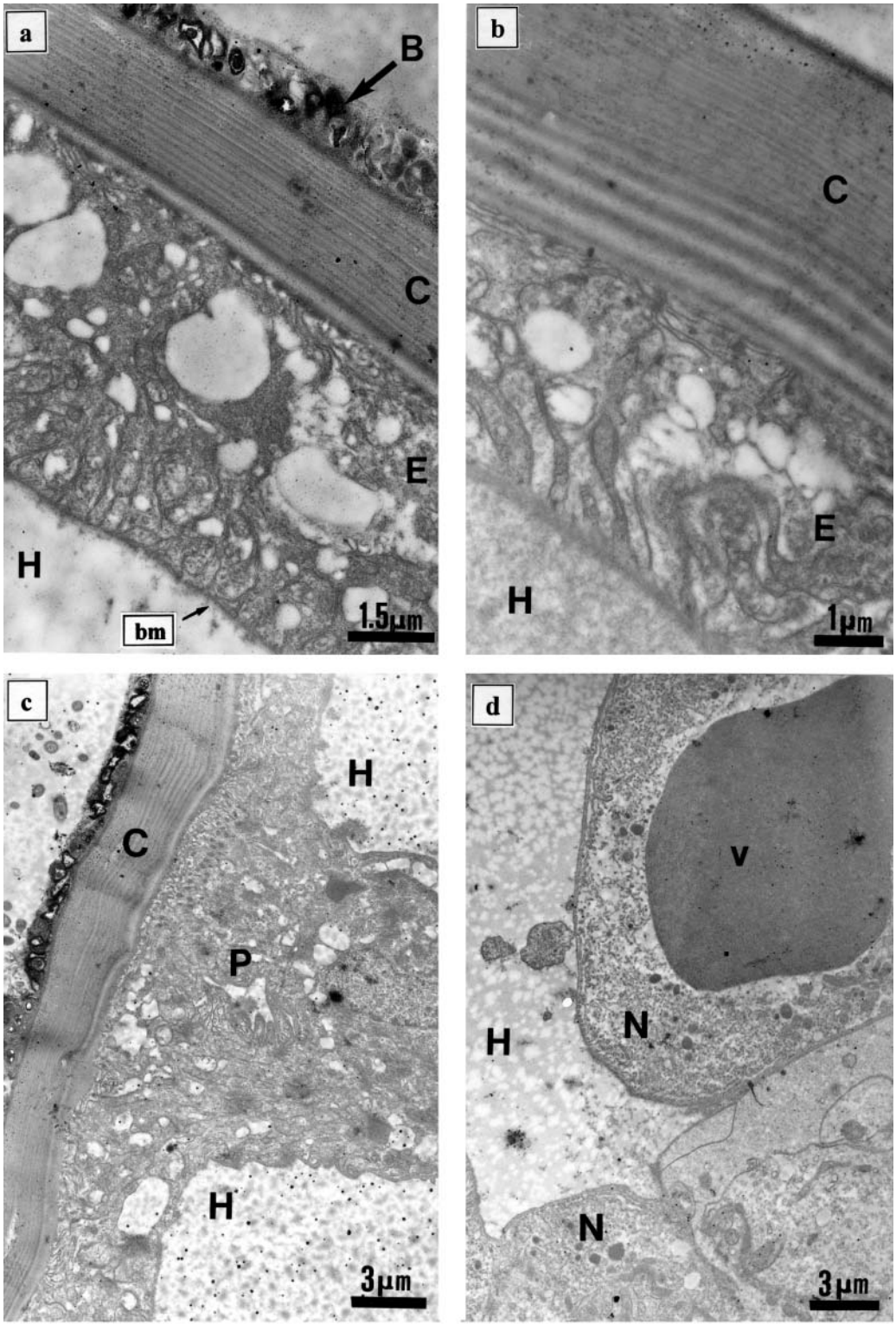

Fig. 4. *Carcinus maenas*. Electron microscopic sections of gill lamellae from uncontaminated control crabs preincubated in sodium selenide and submitted to autometallographic treatment. Only scarce and homogeneously distributed silver grains are visible. (a,b) Cuticle and gill epithelium. An algal biofilm is present on the external side of the cuticule in (a) but not in (b). A multilayered endocuticle is well developed in (b) but not in (a). (c) A pillar cell anchored on the cuticle lined by an algal biofilm. (d) A cluster of nephrocytes with a large central vacuole and peripheral lining of finger-like processes, or pedicels. (B, biofilm; C, cuticle; E, epithelium; H, hemolymph space; bm, basement membrane; N, nephrocyte; P, pillar cell; V, central vacuole of the nephrocyte)

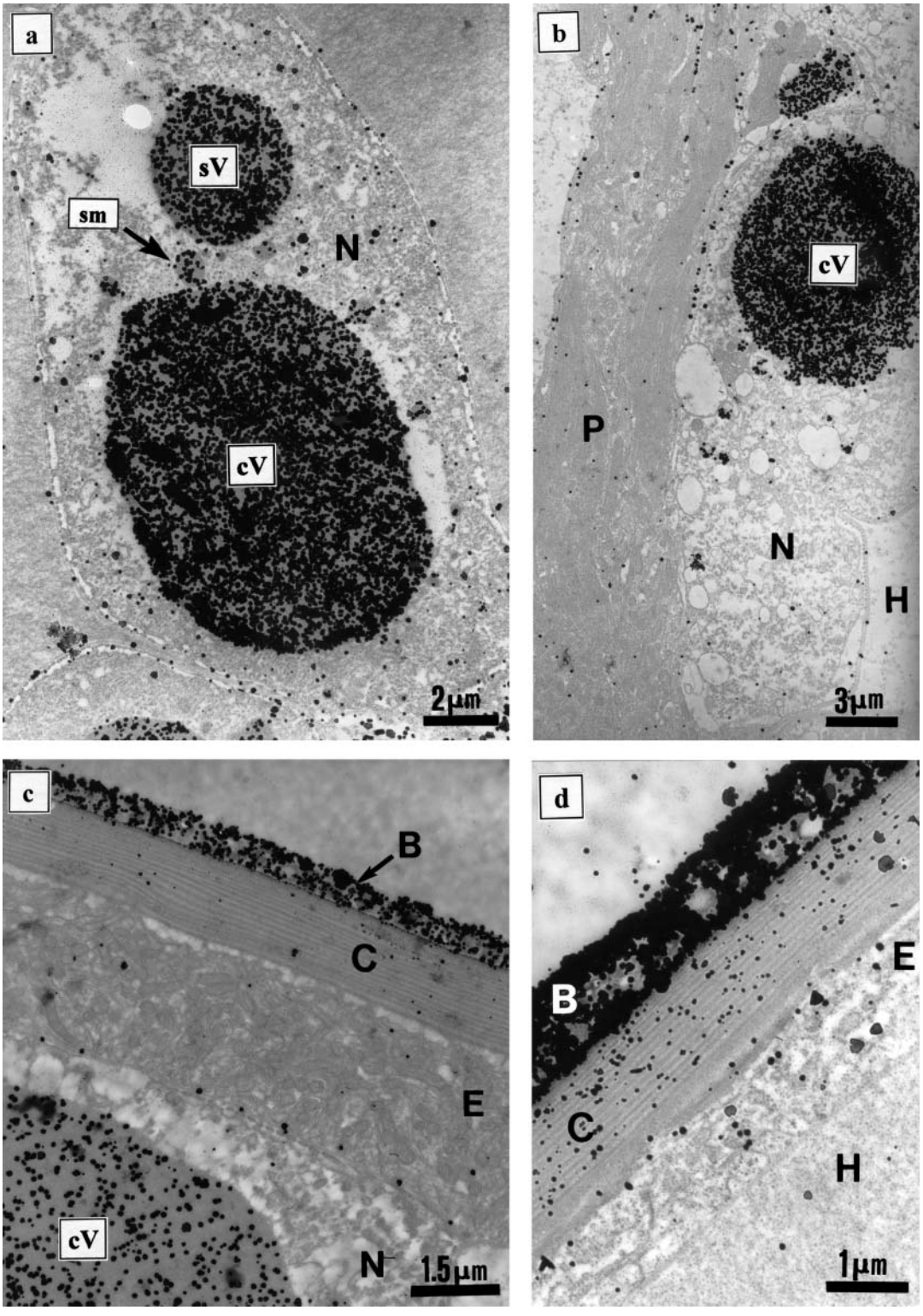

Fig. 5. *Carcinus maenas.* Autometallographic treatment of electron microscopic sections of gill lamellae from crabs contaminated by 2 h exposure to inorganic mercury (50 µg l^{-1}), preincubated in sodium selenide. (a) A nephrocyte with heavily labelled central and satellite vacuoles. Smaller vacuoles in the process of fusion with larger ones are also labelled. (b) A nephrocyte and a poorly labelled pillar cell. (c,d) Lamellar epithelium and cuticle covered by an intensely labelled biofilm. (B, biofilm; C, cuticle; E, epithelium; H, hemolymph space; N, nephrocyte; P, pillar cell; cV, central vacuole of the nephrocyte; sV, satellite vacuole; sm, small labelled vacuole)

uted. This slight reaction may result from the presence of very low natural levels of mercury and also probably from non-specific detection of other metals such as zinc, cadmium or copper.

Fig. 5 displays the results of an autometallographic treatment applied to gills of crabs exposed for 2 h to inorganic mercury (50 µg l^{-1}). Intense staining is seen at 2 locations. First, highly concentrated silver deposits are revealed in the central vacuole of nephrocytes (Fig. 5a,b,c), some smaller vacuoles also being labelled (Fig. 5a), while the cytoplasm of these cells displays only scarce silver grains. Clearly, the dense globular deposits seen by light microscopy (Figs. 2c,d & 3c,d) correspond to these nephrocyte vacuoles, as indicated by their size and location. Second, dark precipitates are also located on the surface of the lamellae, mainly associated with the bacterio-algal biofilm (Fig. 5c,d) and to a lesser extent with the epicuticle. The density of the granules is much lower in the exo- and endocuticle, and all other internal structures such as epithelial (Fig. 5c) and pillar cells (Fig. 5b) show only scarce silver grains, indicating weak mercury accumulation.

After contamination with methylmercury (50 µg l^{-1}), the autometallographic reaction appears, on the whole, less intense than that observed following exposure of the same duration to the inorganic form of the metal (Fig. 6). Less dense silver grains are seen in the central vacuole of nephrocytes (Fig. 6b) or in the lamellar biofilm (Fig. 6d). When the biofilm is absent, the epicuticle appears well marked (Fig. 6c). In addition, a generally more homogenous distribution of the autometallographic reaction, with for example abundant silver grains in the cytoplasm of nephrocytes (Fig. 6b) and pillar cells (Fig. 6a), indicates a more diffuse distribution of accumulated mercury in the gills.

DISCUSSION

The gill of crustaceans is located in a key physiological position in connection with contamination from the surrounding water. The large area of this organ presents a biological barrier between the polluted medium and the internal compartments, thus conditioning the uptake of mercury by the animal. The results of our mercury analyses illustrate the rapidity and efficiency of gill contamination in crabs. The relatively high metal concentration (50 µg l^{-1}) and short exposure time (2 h) used for the present study were deliberately chosen to match the conditions of limited survival acceptable for the *in vitro* preparation. At this ambient level and despite the very short exposure time, concentrations of mercury found in gill tissue were similar *in vivo* and *in vitro* and approached those measured in a previous study (Laporte et al. 1997) in which exposure duration (15 d) and contaminant metal level (1 µg l^{-1}) were ecologically more realistic. These concentrations are also of the same order of magnitude as those reported for other crustacean species, shrimp (Andersen & Baatrup 1988) or Norway lobster (Canli & Furness 1995). In addition, our experiments, as well as our previous results showing a huge mercury bioconcentration in gill compared to other tissues (Laporte et al. 1997), clearly indicate that the gill barrier can considerably limit the contamination of other internal organs thanks to a strong binding of the accumulated metal. Indeed, using the perfused gill technique, we have shown that the portion of mercury entering the gill that successfully crosses the different cellular layers to reach the circulatory system is very low compared to the portion that stays trapped in the gill tissue. Following 2 h exposure to 50 µg Hg l^{-1} of inorganic or methylmercury, only 1.2% and 0.7% of the total metal uptake into the gills was recovered in the perfusion medium. The gills are thus a very effective barrier that is able, in the conditions of our contamination protocol, to retain about 99% of the inorganic or methylated mercury entering the body. Whether the efficiency of this barrier declines as the accumulation sites become saturated is not known but is obviously worthy of investigation. It should also be stressed that the present data were obtained using only posterior gills which were easier to perfuse. It is well known in euryhaline crabs that posterior gills are involved in ion transport, while the much simpler anterior gills are thought to be mainly associated with respiratory gas exchange (Compère et al. 1989, Taylor & Taylor 1992). Although a comparison between anterior and posterior gills would obviously be of interest, our previous data showing nearly identical high levels of metal bioaccumulation (Laporte et al. 1997) might suggest a similar behavior of both types of gills towards mercury uptake.

That the gills are a route for trace metal uptake is easily explained taking into account their high surface/volume ratio and the intense convection of water on their external side as well as of hemolymph on their internal side. For this reason, gill tissue has also been considered to be very sensitive to metal toxic action, this leading often to well-characterized cytological damages (Bubel 1976, Mallatt 1985, Lauren 1991, Nonnotte et al. 1993, Lawson et al. 1994, Pawert et al. 1998) as well as functional impairment of ionic and respiratory gas exchanges (Spicer & Weber 1991). Whether this could be related to the ability of the gills to retain a very important part of the metal they take up remains to be established. However, amounts of mercury measured in the gills in this and other studies seem of the same order of magnitude as those usually considered to induce toxicity (Clarkson 1994, Niimi & Kissoon 1994, Wiener & Spry 1996); this raises the question of the nature and location of the

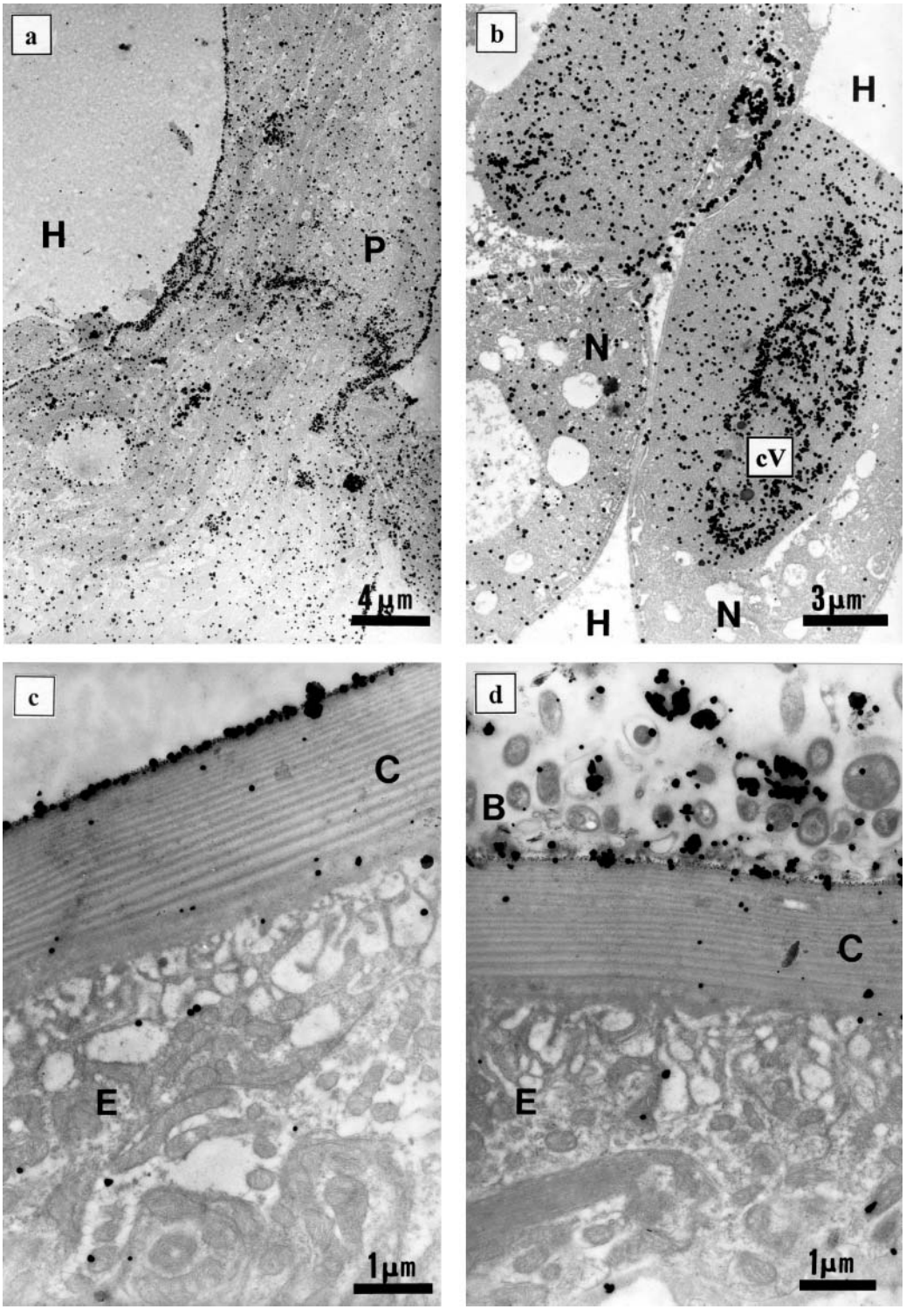

Fig. 6. *Carcinus maenas.* Autometallographic treatment of electron microscopic sections of gill lamellae from crabs contaminated by 2 h exposure to methylmercury (50 µg l^{-1}), preincubated in sodium selenide. (a) A pillar cell with homogeneously distributed silver grains. (b) A cluster of nephrocytes. Homogeneously distributed silver grains are visible in the cytoplasm. The central vacuole is clearly more labelled than the cytoplasm but silver grains are less dense than in crabs contaminated with inorganic mercury (see Fig. 5a,b). (c) Epithelium and cuticle without a biofilm. The epicuticle only is clearly labelled. (d) Epithelium and cuticule covered with an algal biofilm the labelling of which is clearly less dense than in crabs contaminated with inorganic mercury (see Fig. 5c,d). (B, biofilm; C, cuticle; E, epithelium; H, hemolymph space; N, nephrocyte; P, pillar cell; cV, central vacuole of the nephrocyte)

accumulated metal within the different cellular compartments of the gill.

Our present observations use both conventional light and transmission electron microscopy to locate accumulated mercury in gill tissue of the shore crab and thus may contribute to explaining the very high ability of gill tissue to retain the 2 chemical forms. There are probably a great variety of potential fixation sites for the metal taken up from the water. Indeed, when the animals were contaminated with the inorganic form of the metal, some mercury is clearly retained superficially on the cuticular lining of the gill lamellae, but the major deep site of bioaccumulation appears to be the central vacuole of gill nephrocytes. The pattern of accumulation is clearly different when crabs were exposed to methylmercury. Although nephrocytes remain also involved, the metal appears distributed more homogeneously in all gill cellular structures. To the best of our knowledge, this study is the first to use transmission electron microscopy to visualize both inorganic and methylated mercury accumulations by the autometallographic reaction in crustacean gills. The cytological resolution of the technique is highly valuable, but many limitations still remain. While the specificity of mercury detection seems beyond doubt (Danscher & Møller-Madsen 1985, Skak & Baatrup 1993, Braeckman & Raes 1999), all chemical forms of the metal could not be considered as reactive. If, as classically assumed, only sulfide- and selenide-bound metal atoms could act as catalysts for reduction of Ag^+ ions and deposition of silver grains, the histological detection should depend on the chemical fate of mercury after uptake. This fate is clearly unknown and is probably different according to the chemical forms and species of the contaminating metal, to the particular cytological structures and to the availability of the cellular ligands.

Even with these reservations in mind, our results led to some clear-cut conclusions, with good consistency between observations by light and electron microscopy: (1) the dense globular silver deposits seen by light microscopy within the lamellar septum and gill shaft correspond to the central vacuole of nephrocytes; (2) by both techniques, large amounts of the metal appear also trapped on the cuticular biofilm after contamination with inorganic mercury, but much less with methylmercury. This agrees with a study by Lawson & Mason (1998) showing that inorganic mercury is readily retained in the pecto-cellulosic cell wall of unicellular algae, while the organic form appears quickly taken up. Braeckman et al. (1998) demonstrated a similar distribution pattern of both compounds in insect cell cultures. Moreover, using autoradiography to reveal bioaccumulated Hg in the beetle, Lindqvist et al. (1995) found that methylmercury is evenly distributed in most body tissues, whereas inorganic mercury stays confined to the interface organs. The respective part of mercury taken up in the gill tissue and that adsorbed on the biofilm could not be quantified in the present study. As the algal coat is well known to be variable according to the stage of the molt cycle (Goodman & Cavey 1990), this could concomitantly result in large differences in mercury uptake and storage.

Accumulation in the nephrocyte vacuole is particularly spectacular, especially after inorganic mercury contamination. Cells of this type are found in various tissues of many invertebrate groups: molluscs, arthropods, echinoderms, ascidians, etc. (Meyhoefer et al. 1985, Welsch & Rehkaemper 1987, Meyhofer & Morse 1996, Lambert et al. 1998). Their role in the storage and/or detoxification of heavy metals has been suggested in various aquatic species (Dillaman 1980, Giamberini & Pihan 1996, Soto et al. 1996, Vandenbulcke et al. 1998). The peripheral pedicels of nephrocytes are similar to those of the podocytes of the cells lining the Bowman space in the kidney of vertebrates and through which a plasma ultrafiltrate is formed (Ruppert 1994). Those cells have in fact been shown to accumulate mercury (Baatrup et al. 1986, Wilks et al. 1994) and thus have also been identified as important target sites for Hg-induced nephrotoxicity in vertebrates (Prasada Rao et al. 1989, Bano & Hasan 1990, Artese et al. 1993, Girardi et al. 1996). In crustaceans, nephrocytes have long been considered to be phagocytic (Drach 1930, Doughtie & Rao 1981, Smith & Ratcliffe 1981, Taylor & Taylor 1992), ridding the hemolymph of any cell debris or foreign substances. Recent studies seem also to demonstrate an ultrafiltration function in those crustacean cells (Johnson 1987, Ueno et al. 1997, Maina 1998). The mechanism(s) behind the internalization of mercury, and most probably other heavy metals, is not known, but the obvious presence of silver grains in small inclusions ready to fuse with the large central vacuole (see Fig. 5a, b) strongly suggests endocytosis as the accumulation process. Interestingly, Mason et al. (1984) have shown that the nephrocytes of *Littorina littorea* specimens collected from clean and polluted sites contain very high intravacuolar concentrations of sulfur. The well-known affinity of mercury for sulfur compounds (Dyrssen & Wedborg 1991) could easily explain the striking capacity of nephrocytes to bioconcentrate this metal. Nevertheless, further studies are still needed to clearly identify the chemical nature of the vacuole content and to establish whether the internalized mercury is present as a non-toxic form. The ultimate fate of mercury trapped in the nephrocytes remains also to be investigated. While metals adsorbed on the surface, or stored in, the gill cuticle can obviously be lost at molt, the possibility of extrusion of metal-loaded nephrocytes,

either at molt or at any other time, remains undocumented. Whatever the fate of the trapped mercury might be, our observations clearly indicate that the nephrocytes allow the gills to act as a very efficient barrier limiting access of the inorganic form of the metal to circulating hemolymph, and thus its distribution to other internal target organs and probably its toxic effects to the organism. It is also important to stress the rapidity of mercury accumulation in the gill. We indeed have observed that for shorter exposure duration (30 min) Hg deposits were already observable not only at the interface of the contaminated medium, i.e. the cuticle, but in the central vacuole of the nephrocytes (results not shown in this paper). Whether this is also the case for longer exposure times, i.e. whether nephrocytes can act as permanent metal stores, is not known but is obviously worthy of investigation.

Contamination with methylmercury led to a much more diffuse distribution of silver grains throughout most of the gill cell structures. This probably reflects a greater mobility of this chemical form in its free diffusion to most body compartments. This is also consistent with the well known higher toxicity of methylmercury in numerous aquatic species (Lock et al. 1981, George 1990, Hall & Anderson 1995, Wright 1995, Jackson 1998). As shown by Mason et al. (1996), these properties cannot solely be explained by liposolubility differences between the 2 chemical forms: the $K_{o/w}$ (octanol/water partitioning coefficient) value for CH_3HgCl is indeed only 1.7 compared to 3.3 for the inorganic species $HgCl_2$. In our experiments, although the gill mercury concentration attained after a 2 h exposure to methylmercury appears significantly higher than after contamination with inorganic mercury (Fig. 1, Table 1), the intensity of the autometallographic reaction is globally less than after contamination with the inorganic compound. This most likely indicates either that the detection of the organic form of the metal is less efficient by the autometallographic reaction or that the metal is not really detected as methylmercury, which might have been at least partly demethylated after uptake. That the nephrocyte central vacuole seems more intensely marked than other structures after contamination with organic mercury could also suggest that this form may undergo substantial chemical processing, thus affecting its distribution throughout the gill and its subsequent detection.

In conclusion, our study highlights the key position of the crustacean gill in connection with mercury exposure from the surrounding medium. The gill tissue shows a striking ability to retain both inorganic and methylated forms of the metal and thus to protect the other internal compartments from mercury contamination and subsequent toxicity. The tissular and cellular distributions of both mercuric compounds are markedly different and can only be partly explained by the different chemical characteristics of HgII and MeHg. The fate and the possible toxicity of mercury stored in the nephrocyte remain to be studied.

LITERATURE CITED

Andersen JT, Baatrup E (1988) Ultrastructural localization of mercury accumulations in the gills, hepatopancreas, midgut, and antennal glands of the brown shrimp, *Crangon crangon*. Aquat Toxicol 13(4):309–324

Artese L, Boscolo P, Carmignani M, Felaco M, Carelli G, Sacchettonilogroscino G, Grilli A, Giuliano G (1993) Morphological patterns in rats with glomerulonephritis induced by long-term exposure to mercury. Int J Immunopathol Pharmacol 6(2):99–108

Baatrup E, Doving KB (1990) Histochemical demonstration of mercury in the olfactory system of salmon (*Salmo salar* L.) following treatments with dietary methylmercuric chloride and dissolved mercuric chloride. Ecotoxicol Environ Saf 20(3):277–289

Baatrup E, Nielsen MG, Danscher G (1986) Histochemical demonstration of two mercury pools in trout tissues: mercury in kidney and liver after mercuric chloride exposure. Ecotoxicol Environ Saf 12(3):267–282

Bano Y, Hasan M (1990) Histopathological lesions in the body organs of cat-fish (*Heteropneustes fossilis*) following mercury intoxication. J Environ Sci Health Part B Pestic Food Contam Agric Wastes 25(1):67–85

Barradas C, Pequeux A (1996) Uptake of mercury by the gills of the fresh water Chinese crab *Eriocheir sinensis* (Milne-Edwards). Comp Biochem Physiol C 113(2):157–160

Bianchini A, Gilles R (1996) Toxicity and accumulation of mercury in three species of crabs with different osmoregulatory capacities. Bull Environ Contam Toxicol 57(1): 91–98

Boudou A, Ribeyre F (1998) Mercury in the food web: accumulation and transfer mechanisms. In: Sigel A, Sigel H (eds) Mercury and its effects on environment and biology. Metal ions in biological systems, 34. M. Dekker, New York, p 289–319

Braeckman B, Raes H (1999) The ultrastructural effect and subcellular localization of mercuric chloride and methylmercuric chloride in insect cells (*Aedes albopictus* C6/36). Tissue Cell 31(2):223–232

Braeckman B, Cornelis R, Rzeznik U, Raes H (1998) Uptake of $HgCl_2$ and MeHgCl in an insect cell line (*Aedes albopictus* C6/36). Environ Res 79(1):33–40

Bubel A (1976) Histological and electron microscopical observations on the effects of different salinities and heavy metal ions on the gills of *Jaera nordmanni* (Rathke) (Crustacea, Isopoda). Cell Tissue Res 167:65–95

Canli M, Furness RW (1995) Mercury and cadmium uptake from seawater and from food by the Norway lobster *Nephrops norvegicus.* Environ Toxicol Chem 14(5): 819–828

Clarkson TW (1994) The toxicology of mercury and its compounds. In: Watras CJ, Huckabee JW (eds) Mercury pollution: integration and synthesis. Lewis Publishers, Chelsea, p 631–640

Compère P, Wanson S, Pequeux A, Gilles R, Goffinet G (1989) Ultrastructural changes in the gill epithelium of the green crab *Carcinus maenas* in relation to external salinity. Tissue Cell 21(2):299–318

Danscher G (1984) Autometallography: a new technique for light and electron microscopic visualization of metals in biological tissues (gold, silver, metal sulfides and metal selenides). Histochemistry 81:331–335

Danscher G, Møller-Madsen B (1985) Silver amplification of mercury sulfide and selenide: a histochemical method for light and electron microscopic localization of mercury in tissue. J Histochem Cytochem 33:219–228

Danscher G, Stoltenberg M, Juhl S (1994) How to detect gold, silver and mercury in human brain and other tissues by autometallographic silver amplification. Neuropathol Appl Neurobiol 20(5):454–467

Dillaman RM (1980) Toxicity of cadmium to *Helisoma anceps* and its effect on kidney ultrastructure. J Invertebr Pathol 36(2):223–234

Doughtie DG, Rao KR (1981) The syncytial nature and phagocytic activity of the branchial podocytes in the grass shrimp, *Palaemonetes pugio*. Tissue Cell 13(1): 93–104

Drach P (1930) Etude sur le système branchial des Crustacés Décapodes. Arch Anat Microsc Morphol Exp 26:83–133

Dyrssen D, Wedborg M (1991) The sulphur-mercury(II) system in natural waters. Water Air Soil Pollut 56:507–519

George SG (1990) Biochemical and cytological assessments of metal toxicity in marine animals. In: Furness RW, Rainbow PS (eds) Heavy metals in the marine environment. CRC Press, Boca Raton, p 124–142

Giamberini L, Pihan JC (1996) The pericardial glands of the zebra mussel: ultrastructure and implication in lead detoxication process. Biol Cell 86(1):59–65

Girardi G, Saball DE, Salvarrey MS, Elias MM (1996) Glomerular compromise in mercuric chloride-induced nephrotoxicity. J Biochem Toxicol 11(4):189–196

Goodman SH, Cavey MJ (1990) Organization of a phyllobranchiate gill from the green shore crab *Carcinus maenas* (Crustacea, Decapoda). Cell Tissue Res 260:495–505

Hall LW Jr, Anderson RD (1995) The influence of salinity on the toxicity of various classes of chemicals to aquatic biota. Crit Rev Toxicol 25(4):281–346

Jackson TA (1991) Biological and environmental control of mercury accumulation by fish in lakes and reservoirs of northern Manitoba, Canada. Can J Fish Aquat Sci 48(12): 2449–2470

Jackson TA (1998) Mercury in aquatic ecosystems. In: Langston WJ, Bebianno MJ (eds) Metal metabolism in aquatic environments. Chapman & Hall, London, p 77–158

Johnson PT (1987) A review of fixed phagocytic and pinocytotic cells of decapod crustaceans, with remarks on hemocytes. Dev Comp Immunol 11(4):679–704

Jones RD, Jacobson ME, Jaffe R, West-Thomas J, Arfstrom C, Alli A (1995) Method development and sample processing of water, soil, and tissue for the analysis of total and organic mercury by cold vapor atomic fluorescence spectrometry. Water Air Soil Pollut 80(1–4):1285–1294

Lambert CC, Lambert G, Crundwell G, Kantardjieff K (1998) Uric acid accumulation in the solitary ascidian *Corella inflata*. J Exp Zool 282(3):323–331

Laporte JM, Ribeyre F, Truchot JP, Boudou A (1996) Experimental study of the combined effects of pH and salinity on the bioaccumulation of inorganic mercury in the crayfish *Astacus leptodactylus*. Chem Speciat Bioavailab 8(1–2): 1–15

Laporte JM, Truchot JP, Ribeyre F, Boudou A (1997) Combined effects of water pH and salinity on the bioaccumulation of inorganic mercury and methylmercury in the shore crab *Carcinus maenas.* Mar Pollut Bull 34(11):880–893

Lauren DJ (1991) The fish gill: a sensitive target for waterborne pollutants. In: Mayes MA, Barron MG (eds) Aquatic toxicology and risk assessment. ASTM, Philadelphia, p 223–244

Lawson NM, Mason RP (1998) Accumulation of mercury in estuarine food chains. Biogeochemistry 40(2–3):235–247

Lawson SL, Jones MB, Moate RM (1994) Structural variability and distribution of cells in a posterior gill of *Carcinus maenas* (Decapoda, Brachyura). J Mar Biol Assoc UK 74(4): 771–785

Lindqvist L, Block M, Tjalve H (1995) Distribution and excretion of Cd, Hg, methyl-Hg and Zn in the predatory beetle *Pterostichus niger* (Coleoptera, Carabidae). Environ Toxicol Chem 14(7):1195–1201

Lock RAC, Cruijsen MJM, Van Overbeeke AP (1981) Effects of mercuric chloride and methylmercuric chloride on the osmoregulatory function of the gills in rainbow trout, *Salmo gairdneri* Richardson. Comp Biochem Physiol C 68:151–159

Maina JN (1998) Locations, ultrastructural morphology, and putative functions of the branchial podocytes of the fresh water crab *Potamon niloticus* Savigny (Crustacea, Decapoda, Potamonidae). Tissue Cell 30(5):562–572

Mallatt J (1985) Fish gill structural changes induced by toxicants and other irritants: a statistical review. Can J Fish Aquat Sci 42(4):630–648

Marigomez I, Orbea A, Olabarrieta I, Etxeberria M, Cajaraville MP (1996) Structural changes in the digestive lysosomal system of sentinel mussels as biomarkers of environmental stress in mussel-watch programmes. Comp Biochem Physiol C 113(2):291–297

Mason AZ, Simkiss K, Ryan KP (1984) The ultrastructural localization of metals in specimens of *Littorina littorea* collected from clean and polluted sites. J Mar Biol Assoc UK 64:699–720

Mason RP, Reinfelder JR, Morel FMM (1996) Uptake, toxicity, and trophic transfer of mercury in a coastal diatom. Environ Sci Technol 30(6):1835–1845

McLusky DS, Bryant V (1986) The effect of temperature and salinity on the toxicity of heavy metals to marine and estuarine invertebrates. Oceanogr Mar Biol Annu Rev 24: 481–520

Meyhofer E, Morse MP (1996) Characterization of the bivalve ultrafiltration system in *Mytilus edulis*, *Chlamys hastata*, and *Mercenaria mercenaria*. Invertebr Biol 115(1): 20–29

Meyhoefer E, Morse MP, Robinson WE (1985) Podocytes in bivalve molluscs: Morphological evidence for ultrafiltration. J Comp Physiol B 156(2):151–161

Morel FMM, Kraepiel AML, Amyot M (1998) The chemical cycle and bioaccumulation of mercury. Annu Rev Ecol Syst 29:543–566

Newman GR, Jasani B (1998) Silver development in microscopy and bioanalysis: Past and present. J Pathol 186(2):119–125

Niimi AJ, Kissoon GP (1994) Evaluation of the critical body burden concept based on inorganic and organic mercury toxicity to rainbow-trout (*Oncorhynchus mykiss*). Arch Environ Contam Toxicol 26(2):169–178

Nonnotte L, Boitel F, Truchot JP (1993) Waterborne copper causes gill damage and hemolymph hypoxia in the shore crab *Carcinus maenas*. Can J Zool 71(8):1569–1576

Parkman H, Meili M (1993) Mercury in macroinvertebrates from Swedish Forest Lakes—influence of lake type, habitat, life cycle, and food quality. Can J Fish Aquat Sci 50(3): 521–534

Pawert M, Muller E, Triebskorn R (1998) Ultrastructural changes in fish gills as biomarker to assess small stream pollution. Tissue Cell 30(6):617–626

Pequeux A, Bianchini A, Gilles R (1996) Mercury and osmoregulation in the euryhaline crab, *Eriocheir sinensis*. Comp Biochem Physiol C 113(2):149–155

Pierrot C, Pequeux A, Thuet P (1995) Perfusion of gills isolated from the hyper-hyporegulating crab *Pachygrapsus marmoratus* (Crustacea, Decapoda)—adaptation of a method. Arch Physiol Biochem 103(4):401–409

Prasada Rao PVV, Jordan SA, Bhatnagar MK (1989) Ultrastructure of kidney of ducks exposed to methylmercury, lead and cadmium in combination. J Environ Pathol Toxicol Oncol 9(1):19–44

Ruppert EE (1994) Evolutionary origin of the vertebrate nephron. Am Zool 34(4):542–553

Skak C, Baatrup E (1993) Quantitative and histochemical demonstration of mercury deposits in the inner ear of trout, *Salmo trutta*, exposed to dietary methylmercury and dissolved mercuric chloride. Aquat Toxicol 25(1–2): 55–70

Smith VJ, Ratcliffe NA (1981) Pathological changes in the nephrocytes of the shore crab, *Carcinus maenas*, following injection of bacteria. J Invertebr Pathol 38(1):113–121

Soto M, Cajaraville MP, Marigomez I (1996) Tissue and cell distribution of copper, zinc and cadmium in the mussel, *Mytilus galloprovincialis*, determined by autometallography. Tissue Cell 28(5):557–568

Soto M, Quincoces I, Marigomez I (1998) Autometallographical procedure for the localization of metal traces in molluscan tissues by light microscopy. J Histotechnol 21(2):123–127

Spicer J, Weber RE (1991) Respiratory impairment in crustaceans and molluscs due to exposure to heavy metals. Comp Biochem Physiol C 100(3):339–342

Stein ED, Cohen Y, Winer AM (1996) Environmental distribution and transformation of mercury compounds. Crit Rev Environ Sci Technol 26:1–43

Suedel BC, Boraczek JA, Peddicord RK, Clifford PA, Dillon TM (1994) Trophic transfer and biomagnification potential of contaminants in aquatic ecosystems. Rev Environ Contam Toxicol 136:21–89

Taylor HH, Taylor EW (1992) Gills and lungs: the exchange of gases and ions. In: Harrison FW, Humes AG (eds) Microscopic anatomy of invertebrates: decapod Crustacea. Wiley-Liss, New York, p 204–293

Ueno M, Inoue Y, Niwa N (1997) Podocytes of the freshwater shrimp—fine structure and effect of injected trypan blue. J Electron Microsc 46(6):485–490

Vandenbulcke F, Grelle C, Fabre MC, Descamps M (1998) Ultrastructural and autometallographic studies of the nephrocytes of *Lithobius forficatus* L. (Myriapoda, Chilopoda): role in detoxification of cadmium and lead. Int J Insect Morphol Embryol 27(2):111–120

Welsch U, Rehkaemper G (1987) Podocytes in the axial organ of echinoderms. J Zool 213(1):45–50

Wiener JG, Spry DJ (1996) Toxicological significance of mercury in freshwater fish. In: Beyer WN, Heinz GH (eds) Environmental contaminants in wildlife: interpreting tissue concentrations. Lewis Publishers, Boca Raton, p 297–339

Wilks MF, Gregg NJ, Bach PH (1994) Metal accumulation and nephron heterogeneity in mercuric chloride-induced acute renal failure. Toxicol Pathol 22(3):282–290

Wright DA (1995) Trace metal and major ion interactions in aquatic animals. Mar Pollut Bull 31(1–3):8–18

Editorial responsibility: Otto Kinne (Editor), Oldendorf/Luhe, Germany

Submitted: March 19, 2001; Accepted: July 10, 2001
Proofs received from author(s): March 18, 2002